MASTER COPY KEEP THIS COPY FOR REPRODUCTION PURPOSES

AD-A264 264

TION PAGE

1.	3. REPORT TYPE AND DATES COVERED
	Reprint

4. TITLE AND SUBTITLE

Title shown on Reprint

5. FUNDING NUMBERS

DAAL03-91-G-0340

6. AUTHOR(S)

Author(s) listed on Reprint

7. PERFORMING ORGANIZATION NAME(S) AND ADDRESS(ES)

Howard Univ.
Washington, D.C. 20059

8. PERFORMING ORGANIZATION REPORT NUMBER

9. SPONSORING/MONITORING AGENCY NAME(S) AND ADDRESS(ES)

U. S. Army Research Office
P. O. Box 12211
Research Triangle Park, NC 27709-2211

10. SPONSORING/MONITORING AGENCY REPORT NUMBER

ARO 29671.1-MS-H

11. SUPPLEMENTARY NOTES

The view, opinions and/or findings contained in this report are those of the author(s) and should not be construed as an official Department of the Army position, policy, or decision, unless so designated by other documentation.

12a. DISTRIBUTION/AVAILABILITY STATEMENT

Approved for public release; distribution unlimited.

12b. DISTRIBUTION CODE

13. ABSTRACT (Maximum 200 words)

ABSTRACT ON REPRINT

14. SUBJECT TERMS			15. NUMBER OF PAGES
			16. PRICE CODE
17. SECURITY CLASSIFICATION OF REPORT	18. SECURITY CLASSIFICATION OF THIS PAGE	19. SECURITY CLASSIFICATION OF ABSTRACT	20. LIMITATION OF ABSTRACT
UNCLASSIFIED	UNCLASSIFIED	UNCLASSIFIED	UL

RAMAN AND X-RAY SCATTERING FROM DENSE SEMICONDUCTOR-DIELECTRIC NANOCOMPOSITES

W.H. YANG*#, T.E. HUBER*&, J.A. LUBIN*, G.E. WALRAFEN*, AND C.A. HUBER@
*Laser Chemistry, Howard University, Washington, DC 20059
#Chinese Academy of Sciences, Beijing, People's Republic of China
&Department of Physics, Polytechnic University, Brooklyn, NY 11201
@Naval Surface Warfare Center, Code R36, Silver Spring, MD 20903

ABSTRACT

Raman scattering measurements have been performed on semiconductor-insulator nanocomposites in which the semiconducting phase occupies a significant (30%) volume fraction. The composites have been synthesized by high pressure injection of the conducting melt into the nanochannels of commercially available insulating matrices. The optical phonon spectra of GaSb- and Te-SiO_2 composites exhibit shifts, broadenings, and asymmetries when compared to those of the semiconducting bulk. These are interpreted in terms of strains and phonon confinement in the microcrystalline semiconducting phase. X-ray diffraction measurements allow us to correlate the effects of crystallite size and strains on the optical modes of the composites.

INTRODUCTION

Composites of more than one solid phase in which the heterogeneity length scale is in the nanometer range represent a regime intermediate between the molecular and bulk solid states. As a result of finite size and surface effects, their physical properties are quite different from those of the bulk constituents. In particular, nanocomposites consisting of semiconductors finely dispersed in an insulating matrix represent a dramatic example of how the properties of the semiconducting phase are modified by processing. Among such, the quantum confinement of carriers and the local electric field discontinuity at the interface between the two phases can lead to large enhancements of the nonlinear optical response of the composite.[1] This has motivated intensive research on semiconductor nanocrystals synthesized in solid insulating matrices or in colloidal form, or by deposition on a substrate.[2] Most of these syntheses result in a fractional volume of the semiconducting phase of typically less than 1%, yet for many applications higher concentrations are desirable.

We have synthesized semiconductor-insulator nanocomposites in which the semiconducting phase occupies a significant (about 30%) volume fraction. They have been prepared by high pressure injection of the conducting melt into the interconnected, nanometer-size channels of commercially available insulating matrices. The transport and optical properties of the composites are anticipated to be strongly dependent on the connectivity and crystalline state of the semiconducting phase. Raman spectroscopy is a non-destructive technique which has proved to be most useful for the study of the vibrational and structural properties of microcrystalline materials.[3] It has recently been applied with equal success to low-dimensional semiconductor systems, including nanoparticles synthesized in a solid matrix,[4-6] in colloidal form,[6-8] and condensed from the gas phase.[9-10] We here report on Raman scattering and X-ray diffraction (XRD)

Mat. Res. Soc. Symp. Proc. Vol. 286. ©1993 Materials Research Society

measurements on dense semiconductor nanocomposites. Correlation between the results from both types of measurements allows us to characterize the microstructure of this new class of materials.

EXPERIMENT

Nanocomposites have been prepared by high pressure injection of molten semiconductors into nanochannel silica and alumina matrices of 25%-35% porosity. An externally applied pressure is required to overcome surface tension effects which prevent the semiconductor from entering the narrow channels. Details about the injection apparatus and about the sample preparation process have been reported previously.[11] Briefly, the semiconductor is heated above its melting point and is then pushed inside the matrix channels by a hydrostatic pressure of a few kilobars. When the injection is complete the temperature is lowered and the semiconductor solidifies inside the matrix, the pressure is then released. Dense nanocomposites with a highly reproducible microstructure are obtained in this way since the impregnate copies to a large extent the channel structure of the matrix. Small-angle X-ray scattering measurements (SAXS) show that the microstructure of the porous matrix is not significantly modified by the high temperature-high pressure injection process.[12]

We will specifically discuss composites synthesized from a nanochannel silica of the Vycor type (Corning 7930). This high content (95%) silica glass is prepared by a phase separation/leaching process which results in a three dimensional, isotropic, interconnected network of channels. From standard nitrogen adsorption porosimetry measurements performed on the porous silica we obtain an average channel diameter of 56 Å, a channel size distribution half width of 10 Å, and a 33% porosity. Although the Vycor channel structure is quite intricate, its narrow pore-size distribution has made it a material of choice for numerous studies of adsorbates and confined fluids. As a consequence, it is by now a fairly well characterized host from which novel composites can be prepared and subsequently investigated. The results of XRD and Raman scattering measurements on composites of selenium, tellurium, and gallium antimonide, are presented in continuation. The choice of these semiconductors is based on their relatively low melting point which simplifies their preparation and, in the case of Te and GaSb, on their small electron and hole effective masses, which will tend to enhance any electronic confinement that may take place in the nanocomposites.

X-ray diffraction

Theta-two theta scans were carried out in an X-ray diffractometer, the K_α emission from a Cu target was employed. The angular calibration was verified and the instrumental resolution was determined from the position and width of the (111) and (400) diffraction peaks from high quality, single crystal silicon wafers. We find that selenium inside the silica channels is amorphous, consistently with the fact that moderately sized selenium crystals are quite difficult to obtain by standard crystal growth techniques. On the other hand, Te and GaSb retain the crystal structure of the bulk (trigonal and cubic zinc-blende, respectively) and their XRD spectra show unexpectedly narrow peaks (Fig. 1).From the position of the high-angle peaks we obtain values for the lattice constants of the semiconducting phase with a precision of about 0.1 %. The lattice constants relative to the values for the bulk, $\delta a/a$, are listed in Table I. The lattice parameters of Te in the composite are practically the same as in the bulk.

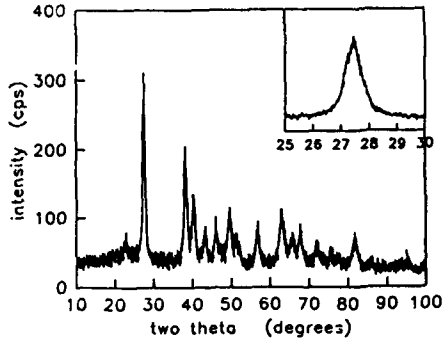

Figure 1. X-ray diffraction spectrum from the Te/SiO_2 composite. The low angle peaks are detailed in the inset.

On the other hand, GaSb in the nanochannels shows an essentially uniform lattice contraction of about $1.5x10^{-3}$. Since the thermal expansion coefficient of bulk GaSb above room temperature is about ten times that of silica ($7.7x10^{-6}$ K^{-1} versus $6x10^{-7}$ K^{-1}) the surrounding matrix will not exert any pressure on the semiconductor from thermal contraction when cooling from the injection temperature of 750 °C to room temperature. The observed lattice contraction may be qualitatively explained by considering that bulk GaSb undergoes a 6% volume expansion at the liquid-to-solid phase transition. Since GaSb is injected inside the channels in its liquid form, it will be confined by the silica walls when the solidus forms and thus may exhibit compressive strains. An additional contribution to the strain may come from the hydrostatic injection pressure of 4 kbar, this would result in a lattice contraction of $2.4x10^{-3}$ if the bulk modulus of GaSb, B= $5.6X10^{11}$ dyn/cm^2, is assumed and the compressive strain remains (i.e., no lattice relaxation takes place) when the pressure is released.

Table I. Semiconductor crystal parameters in the silica composites

	δa/a	D (Å)
Se		amorphous
Te	≤ $1x10^{-3}$	140
GaSb	- $1.5x10^{-3}$	190

An estimate for the average semiconductor crystallite size D can be obtained from the widths of the XRD peaks through Scherrer's equation:

$$D = K\lambda/\beta\cos\theta \qquad (1)$$

where λ is the x-ray wavelength, β is the contribution to the linewidth due to the finite crystallite size, 2θ is the diffraction angle, and K is a factor related to the crystallite shape which could assume values between 0.7 and 1.7 and is taken here to be one.[13] After correcting the measured linewidths for the finite instrumental resolution and for the K_α-doublet broadening, crystallite sizes obtained from peaks corresponding to different sets of crystal planes were found to be about the same, indicating that there is no preferential orientation of the crystallites inside the nanochannels. The values for D listed in Table I were determined from the widths of the low angle peaks, namely the peak at 2θ = 27.48° from the (101) planes in Te and at 25.28° from the (111) planes in GaSb, where K_α-

doublet broadening is minimum. These values represent a lower bound for the crystallite size, since inhomogeneous strains can also contribute to the measured linewidths. The rather small widths observed suggest that there is a significant degree of long range crystalline order, and that the average crystallite size in the composites is not necessarily limited by the 56 Å pore size.

Raman Scattering

For the Raman scattering measurements the composites were polished using standard optical polishing techniques. The 5145 Å line from an Ar ion laser was incident on the sample surface at a 15° angle, the light intensity was kept low enough to avoid sample heating effects. The scattered light was collected in the direction normal to the surface and focused onto the entrance slit of a 0.85 m double monochromator. The instrumental resolution was set at 3.5 cm^{-1}. A cooled GaAs phototube and photon counting electronics were employed. The incident phonon energy of 2.41 eV is much higher than the fundamental energy gap of bulk Te (0.33 eV) and GaSb (0.70 eV).

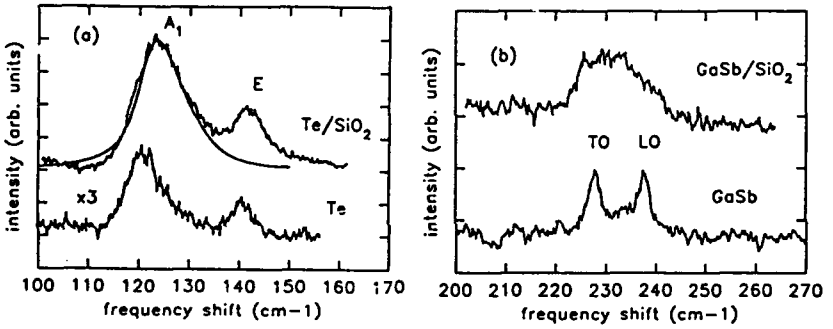

Figure 2. First order Raman spectra of (a): Te/SiO_2, and (b): $GaSb/SiO_2$ composites. The spectra of the bulk semiconductors are also shown. The smooth line fit to the A_1 mode of Te in the composite corresponds to a phonon-confinement calculation as described in the text.

The first order Raman spectra of the Te/SiO_2 composite and of a crystalline sample of bulk Te are shown in Fig 2a. Trigonal Te has three atoms per unit cell arranged in a helix about the c-axis. Consequently, Te has six optical phonon branches , five of which are Raman-active. Only the strongest zone-center modes, the A_1 mode and the high frequency E doublet, are clearly measurable in the experiment. These correspond to symmetric and asymmetric breathing modes of the helical chain, respectively. The Raman peaks of the composite, particularly the strong A_1 mode, show broadenings and high energy shifts and tails when compared to those of bulk Te. Similar broadenings are also observed in the Raman peaks of the GaSb composite (Fig. 2b). In this case, the broadened transverse and longitudinal optical zone-center phonons of zinc-blende GaSb overlap and it becomes difficult to clearly discern any shifts. In the following section we discuss the possible origin of the observed shifts and broadenings of the Raman peaks.

DISCUSSION

We consider two main contributions to the observed Raman line shapes of the

semiconductor nanocrystals namely, strain and phonon confinement effects. Additional effects may come from defects, surfaces, and crystallite size and shape distributions, yet these are more difficult to evaluate with precision.

Strain effects on the phonon frequency ω are described by the Gruneisen parameter:

$$\gamma = - \delta(\ln\omega)/\delta(\ln V) = B\,(\delta\omega/\delta P)/\omega \qquad (2)$$

where V is the crystal volume, B the bulk modulus, and P the hydrostatic pressure. The XRD spectrum of the GaSb composite show the semiconductor nanocrystals to be under a compressive strain $\delta a/a = -1.5\times10^{-3}$. From $\delta a/a = -\delta P/3B$, with $B= 5.6\times10^{11}$ dyn/cm^2 the bulk modulus of bulk GaSb, we obtain $\delta P = 2.5\times10^{9}$ dyn/cm^2 (or 2.5 kbar). The Gruneisen parameter of semiconductor nanocrystals has been found to be very close to that of the bulk for this range of pressures.[6,14] Therefore, using $\gamma= 0.75$ for bulk GaSb we estimate a high energy shift $\delta\omega= 0.8$ cm^{-1} for the optical phonons of GaSb in the composite, too small to be clearly seen in Fig. 2b.

The 2.5 cm^{-1} high energy shift of the A_1 mode of the Te composite (Fig. 2a) can not be explained by strain effects. Bulk Te has a negative Gruneisen parameter, i.e., optical mode frequencies decrease under an applied hydrostatic pressure. From the measured pressure dependence of the A_1 mode of bulk Te, $\delta\omega= -0.64$ cm^{-1}/kbar,[15] a frequency shift of 2.5 cm^{-1} would correspond to a negative (expansive) pressure of 3.9 kbar. Such pressure could be a net pressure resulting from the injection pressure, the pressure from the different thermal expansion of Te and the silica, and the Laplace-type pressure from the surface tension between Te and the silica walls. A hydrostatic pressure of 3.9 kbar would produce a relative change of the lattice constants of Te $\delta a/a= 1\times10^{-2}$ and $\delta c/c= -1.5\times10^{-3}$, much larger than the changes of less than 1×10^{-3} determined from the XRD spectrum of the composite.

We propose that the high energy shifts and asymmetries of the Raman peaks of the Te composite result from phonon confinement in the nanocrystals. For a finite size crystal, localization of the phonon wave function causes the relaxation of the q=0 Raman selection rule, i.e., the phonon wavevector q is not a good quantum number in a finite lattice.[16] This results in contributions to the Raman signal from phonons away from the center of the Brillouin zone. The shift and width of the Raman peaks are then related to the phonon dispersion relation of the material. The A_1 mode of bulk Te shows a strong, positive phonon dispersion relation.[17] The spread in phonon momentum in a Te crystal of size D= 140 Å is $\delta q\approx 2\pi/D \approx 0.1\ q_{BZ}$, with q_{BZ} the zone-edge phonon, and this would produce sizable blue shift of the A_1 Raman peak. On the other hand, the weaker E doublet of bulk Te splits in two modes having a small negative and positive dispersion away from the zone center.[18] Therefore, only a small net effect from phonon confinement may appear on the E mode. Similarly, the LO and TO zone-center phonons of GaSb show only a small negative dispersion.[19]

In the model put forward by Richter et al.16, where the periodic wave function of a phonon in a spherical crystallite of size D is modulated by a confinement function of the type $\exp(-\alpha r^2/D^2)$, the Raman line shape is given by:

$$I(\omega) \propto \int \frac{\exp(-q^2D^2/2\alpha)\ dq}{[\omega - \omega(q)]^2 + (\Gamma_o)^2} \qquad (3)$$

where ω is the frequency shift, $\omega(q)$ the phonon dispersion relation, and Γ_o the natural linewidth. The integration is carried over the Brillouin zone. Using Eq. 3 we have calculated the Raman line shape of the A_1 phonon of Te nanocrystals and fit the result to the spectrum in Fig. 2a. A dispersion relation $\omega(q)= \omega_o + Aq_z^2 + Bq_r^2$, with $\omega_o= 121$ cm^{-1},

A= 453 $cm^{-1}/Å^2$, and B= 120 $cm^{-1}/Å^2$ [17] was employed, and the integration was carried over a cylindrical Brillouin zone. The value Γ_o= 7 cm^{-1}, obtained from the natural linewidth of 6.5 cm^{-1} [18] and the instrumental resolution, was employed. The best fit (Fig. 2a) was obtained for D^2/α = 127. Values for α between 2 and $8\pi^2$ have been reported[3], the latter would correspond to D= 100 Å for our best fit. If cylindrical crystallites are assumed, an equally good fit is obtained for D= 56 Å (the channel diameter of the silica matrix) and α= 2. It does not seem possible then to unambiguously determine the crystallite shape from a fit to the Raman line shape in this circumstance.

SUMMARY

We have examined the structural properties of semiconductor-dielectric nanocomposites synthesized by injection of the conducting melt into nanochannel silica matrices. The Raman scattering spectra show shifts and broadenings which, when combined with results from x-ray diffraction measurements, are interpreted as resulting from phonon confinement in the semiconductor crystallites. The analysis method is currently being extended to nanocomposites consisting of a regular array of semiconductor nanowires prepared from alumina matrices with parallel, cylindrical channels.

This work was supported by the U.S. Army Research Office and by the Naval Surface Warfare Center Independent Research Program.

REFERENCES

1. S. Schmitt-Rink, D.A.B. Miller, and D.S. Chemla, Phys.Rev. **B35**, 8113, 1987.
2. For a review see C. Flytzanis, F. Hache, M.C. Klein, D. Ricard, and Ph. Roussignol, in Progress in Optics, ed. by E. Wolf (Elsevier, New York, 1991), Vol. XXIX.
3. P.M. Fauchet and I.H. Campbell, Critical Rev. in Solid State and Materials Science **14**, S79 (1988).
4. M. Fujii, S. Hayashi, and K. Yamamoto, Appl. Phys. Lett. **57**, 2692 (1990).
5. G. Scamarcio, M. Lugara, and D. Manno, Phys. Rev. **B45**, 3792 (1992).
6. X.S. Zhao, J. Schroeder, P.D. Persans, and T.G. Bilodeau, Phys. Rev. **B43**, 12580 (1991).
7. C.J. Sandroff and L.A. Farrow, Chem. Phys. Lett. **130**, 458 (1986).
8. J.J. Shiang, A.N. Goldstein, and A.P. Alivisatos, J. Chem. Phys. **92**, 3232 (1990).
9. T. Kanata, H. Murai, and K. Kubota, J. Appl. Phys. **61**, 969 (1987).
10. S. Hayashi, H. Sanda, M. Agata, and K. Yamamoto, Phys. Rev. **B40**, 5544 (1989).
11. C.A. Huber and T.E. Huber, J. Appl. Phys. **64**, 6588 (1988).
12. T.E. Huber, P.W. Schmidt, J.-S. Lin, and C.A. Huber, Mat. Res. Soc. Symp. Proc. **EA-25**, 207 (1990), and to be published.
13. H.P. Klug and L.A. Alexander, X-Ray Diffraction Procedures for Polycrystalline and Amorphous Materials, (Wiley, New York, 1954).
14. A.P. Alivisatos, T.D. Harris, L.E. Brus, and A Jayaraman, J. Chem. Phys. **89**, 5979 (1988).
15. W. Richter, J.B. Renucci, and M. Cardona, Phys. Stat. Sol (b) **56**, 223 (1973).
16. R.J. Nemanich and S.A Solin, Phys. Rev. **B20**, 392 (1979); H. Richter, Z.P. Wang, and L. Ley, Solid State Commun. **39**, 625 (1981).
17. W. Richter, in The Physics of Selenium and Tellurium, ed. by E. Gerlach and P. Grosse, Springer Series in Solid State Sciences Vol.13 (Springer, New York, 1979).
18. A.S. Pine and G. Dresselhaus, Phys. Rev. **B4**, 356 (1971).
19. M.K. Farr, J.G. Taylor, and S.K. Sinha, Phys. Rev. **B11**, 1587 (1975).